TRANSIENT RESPONSE OF A FLAP CONTROLLED STOPPED ROTOR

Y. K. Yillikçi *
Istanbul Technical University,
Faculty of Aeronautics and Astronautics
80626 Maslak, Istanbul, TURKIYE

J.V.R. Prasad †and D.P. Schrage ‡
Georgia Institute of Technology,
CERWAT and School of Aerospace Engineering
Atlanta, GA 30332-1500 USA

April 28, 1994

Abstract

A simplified trim procedure coupled with a nonlinear partial differential equation solver is developed for calculating elastic blade tip deflections of a stopped rotor blade during rotor slowing down transition. A conditionally stable explicit finite difference scheme is used to numerically integrate the nonlinear P.D.E's of motion in space and time to obtain the aeroelastic transient response of a hingeless rotor blade with trailing edge flap control. New aerodynamic environment due to flap control is formulated based on Theodorsen's unsteady oscillating airfoil aerodynamics representation including unsteady trailing edge flap motions. Auxillary lift and forward propulsion has been utilized for the chosen micro stopped rotor configuration and different transition flight conditions are considered. Transient blade tip deflections are calculated for these flight conditions.

Nomenclature

$C_{L_{can}}$	auxillary lift coeff. $\frac{L_{can}}{\rho\pi R^4\Omega^2}$
$C_{P_{MR}}$	main rotor power coeff. $\frac{P_{MR}}{\rho\pi R^5\Omega^2}$
$C_{T_{pr}}$	tail propulsion coeff. $\frac{T_{pr}}{\rho\pi R^4\Omega^2}$
$C_{T_{MR}}$	main rotor thrust coeff. $\frac{T_{MR}}{\rho\pi R^4\Omega^2}$
C_W	weight coeff. $\frac{W}{\rho\pi R^4\Omega^2}$
L_v, L_w	lift in v and w directions,
M_ϕ	aerodynamic moment
v, w	elastic deflections
U_P, U_T	velocity components
γ	Lock number
λ_0	rotor induced uniform inflow,
$\Lambda_0, \Lambda_{1S}, \Lambda_{1c}$	flap control inputs
μ	advanced ratio, $\frac{V}{\Omega^2 R}$
σ	solidity, $\frac{bc}{\pi R}$
ϕ	elastic twist (rad)
ϕ	azimuth angle
Ω	rotor speed (rad/sec)

*Asst. Prof, , Formerly UAV Project Coordinator at Undersecretariat For Defense Industries

†Assoc. Professor,

‡Professor and Director of CERWAT and FLIGHT SIM

Presented at 19th ICAS/AIAA Conference, 18-23 September 1994, Anaheim, USA

Introduction

Flap Controlled Rotor Blade Concept

A series of performance, comfort and agility is expected to be achieved by the implementation of rotor active control technology. But practical applications of this technology are still missing due to lack of appropriate rotating blade actuation and active control systems. Smart materials are expected to open new possibilities for the realization of smart rotor blades. Resent studies about present practical applications of smart structures and materials in helicopter active control has been reviewed by Strehlow [1].

The use of swash-plate systems for applying collective and cyclic pitch change has been the primary element of helicopter controls since the earlier phases of its development. Almost today's all rotorcrafts involve swash-plate system as the main control device for adjusting the blade pitch angle in order to balance aerodynamic lift and moment distribution. The application of trailing edge flaps to manipulate rotor blade lift variation was first introduced by Charles Kaman, a distinguished helicopter pionner, and the concept called *servo-flap* was successfully used in several Kaman helicopters.

With the development of advanced sensors, actuators, command-control systems and demand for new technologies for blade control mechanisms; flap and servo-flap control concepts have been started to be analyzed with new objectives. Possible applications of flap controlled rotor systems for Army's High Maneuverability/Agility Rotor Control System (HIMARCS) and conceptual designs of Kaman, Bell and McDonald Douglas (MDHC) helicopter companies have been evaluated detailly in references [2, 3, 4] respectively.

Additional control parameters introduced by flap controls expected to give designers additional flexibilities in tailoring aeroelastic and aerodynamic characteristics of next century's rotor blades. With multi-input flap controls located at outboard section of the blade more efficient blade controls can be achieved with smaller control surfaces. With these expectations complete replacement

of standart pitch control with flap control particularly for a 700 lb micro-helicopter configuration is evaluated and periodic response of an elastic rotor blade with flap control have been analyzed by Yillikci [5]. Tip deflections of the flap controlled elastic blade have been compared with the identical pitch controlled blade. Periodic response characteristics of both control cases are found to be almost identical except for the elastic twist which was obtained higher for the flap controlled blade.

Stopped Rotor Concepts

Stopped rotor concept has been captured the attention of rotorcraft designers for its potential to combine relatively low disk loading rotary wing and higher speed fixed wing flight capabilities. With recently renewed interests NASA has supported a concept evaluation study for alternative VTOL aircraft. McDonald Douglas Helicopter Company (MDHC) completed a series high-speed rotorcraft conceptual design studies for NASA [6] to provide the basis to assess technology needs for the development of these aircraft. One of the two concepts selected as the result of concept evaluation studies for seven different concepts, is the rotor/wing (stopped rotor) configuration. The introduced rotor/wing concept is consisted of a warm cycle, reaction-driven rotor, with a large triangular center body hub and three short-span, wide chord blades. For vertical and low speed flight modes the rotor is powered by ducting mixed flow turbofan engine exhaust gases through the hub and rotor blades out to tip jets. The rotor autorotates during conversion until the aircraft reaches conversion speed and the centerbody is assumed to provide enough lift to achieve 1g conversion. After this conversion the off-loaded rotor becomes a swept forward wing for cruise and high speed flight. By the use of airfoils with blunt leading edge and trailing edges and feathering hinge it is also expected that the need for circulation control will be eliminated.

Similarly a tipjet VTOL Unmanned Air Vehicle UAV concept has been introduced as an alternative UAV vehicle and studies are performed for a 1200 lb shipboard UAV configuration at David Taylor Naval Research and Development Center (DTNRD) [7]. The tipjet UAV is designed to utilize circulation control for lift augmentation during rotary wing mode. A practical application of tipjet VTOL UAV will first require the development of a highly complex air circulation control system which includes fan diffusers, plenums and a series of variable tip and propulsion nozzles.

Servo-flap and flap controls are expected to introduce new alternatives for rotor blade controls. The possibility of complete elimination of swashplate mechanism with the use oftrailing edge flaps along with the utilization of smart actuator/sensor features to rotor blade controls brought an alternative approach for the stopped rotor concept; stopped rotor with flap controls. An initial configuration has been suggested by Kisli [8] and blade dynamics of a stopped rotor with flap controls is also analyzed by Yillikci [9]. Proposed aircraft is assumed to have a lifting surface which will perform as a two bladed helicopter rotor during take-off, low altitude flight and initial climb mode. At a proper forward speed and altitude, rotor will gradually slowed down, still partially loaded. It will be off-loaded after certain rotor speed and brakes will be applied. Rotor blades are assumed to have airfoil sections with blunt leading and trailing edges. Aircraft is utilized with canard and tail wings to generate additional lift for the vehicle during transion and full speed forward flight.

Stopped rotor is also equiped with a auxillary tail propulsion which gradually activated during the rotor slowing down transition. Tail rotor anti-torque force will be replaced mainly by vertical or V shaped tail wings. General configuration of 700 lb ANKA-1 micro-helicopter utilized with flap controlled stopped rotor is selected for numerical calculations. ANKA-1 Micro-Helicopter Project is initiated at Istanbul Technical University, Faculty of Aeronautics and Astronautics and project has been selected by State Planning Office Of Turkiye as a university level design and development project. General configuration of ANKA-1 is shown in Figure 1.

II. Formulation

Formulation of aeroelastic analysis of rotor blades with flap controls is consisted of three major steps. First step of the problem is the formulation and calculation of flap control trim settings for the chosen helicopter configuration. The second step of is the formulation of new aerodynamic environment around the rotor blade. The new set of rotor blade nonlinear partial differential equations are solved numerically as the third step.

Trim Formulations

Rotor slowing down transition mode for the stopped rotor requires a different approach for trim formulation. Since slowing main rotor can no longer maintain the total lift required either a descending and slowing down flight condition or utilization of auxiliary lift and forward propulsion are required to keep the aircraft on its steady flight path. All of these conditions are included to the problem whereas the effects of nonuniform blade geometries are considered.

Required trim parameters for the stopped rotor utilized with flap controls are calculated by an approximate trim formulation. Trim conditions for the pitch control case with the same blade and vehicle configuration are first calculated by the use of standart trim equations given by Johnson [10]. As the second step trim param-

eters directly related with flap control case are recalculated along with the replacement of pitch control with flap control represented up to first harmonics as;

$$\Lambda = \Lambda_0 + \Lambda_{tw}\ r + \Lambda_{1s}\sin\psi + \Lambda_{1c}\cos\psi \qquad (1)$$

where Λ_0 is the collective flap Λ_{tw} is the flap pre-twist, and Λ_{1s} and Λ_{1c}, are first harmonics give once-per variation of the blade trailing edge flap angle.

Sectional blade lift for two-dimensional strip type aerodynamic formulation is written as;

$$\begin{aligned}\frac{F_Z}{\sigma a} = & \frac{1}{2}\left[U_T^2\theta_{ri} - U_P U_T\right] + \left[\frac{c}{4a}(f_2 - f_3)U_T \overset{*}{\Lambda}\right. \\ & - \left.\frac{c^2}{8a}f_4 \overset{**}{\Lambda} + \frac{1}{a}f_1 U_T^2\Lambda\right] \qquad (2)\end{aligned}$$

where θ_{ri} is the rigid pitch angle of the blade, c is the non-dimensional blade chord, Λ is the trailing edge flap angle given by equation 1, a blade lift curve slope and σ is the blade solidity ratio. Parameters f_1, f_2, f_3 and f_4 are related with flap hinge offset geometry which have been introduced by Theodorsen's two-dimensional unsteady aerodynamic formulation for the oscillating airfoils. Detailed expressions of these parameters are given in reference [5].

First term in F_Z formulation is related with blade profile lift with a rigid pitch angle θ_{ri}. Blade sectional velocities U_T and U_P are given in nondimensional form for a rigid blade with only rigid blade flapping motion;

$$U_T = r + \mu\sin\psi$$

$$U_P = \lambda + \overset{*}{\beta}\ r + \beta\mu\cos\psi$$

Resultant blade cross-sectinal velocity is approximated as $U = U_T$. Mean of the total rotor thrust formulated the use of equation 2 as,

$$\begin{aligned}\frac{C_{T_0}}{\sigma a} = & \frac{1}{2}\left(C_{12} + C_{10}\frac{\mu^2}{2}\right)\theta_{ri} - \frac{1}{2}C_{11}\lambda \\ & + + \left(d_{3k2} + d_{3k0}\frac{\mu^2}{2}\right)\Lambda_0 \\ & + \left(d_{3k3} + d_{3k1}\frac{\mu^2}{2}\right)\Lambda_{tw} \\ & + d_{3k1}\mu\Lambda_{1s} - d_{1k0}\frac{\mu}{2}\Lambda_{1c} \qquad (3)\end{aligned}$$

Parameters $C_{10}, C_{11}, ..., d_{3k3}$ are related with blade chord and flap geometries and are given in reference [5]. Equation 3 gives the amount of Λ_0 control input required to maintain the mean of the rotor thrust C_{T_0}.

Rotor blade flapping dynamic equilibrium must be also considered to calculate the required cyclic flap angle inputs Λ_{1s}, Λ_{1c} zeroth harmonic of blade flapping, β_0. Flapping dynamics of a rigid rotor can be written as;

$$\overset{**}{\beta} + \nu^2\,\beta = \frac{1}{2}\frac{\rho c a R^4}{I_b}\int_0^1 r F_Z dr \qquad (4)$$

where blade flapping motion is expressed as up to its first harmonics,

$$\beta = \beta_0 + \beta_{1s}\sin\psi + \beta_{1c}\cos\psi \qquad (5)$$

Equation 4 give three equilibrium conditions when harmonic balance equations up to first harmonics are considered. These equations are written as;

$$\begin{aligned}\frac{\nu^2}{\gamma}\beta_0 & - \left(d_{3k3} + d_{3k1}\frac{\mu^2}{2}\right)\Lambda_0 - d_{3k2}\,\mu\Lambda_{1s} \\ & + C_{12}\frac{\lambda}{2} - \left(d_{3k4} + d_{3k2}\frac{\mu^2}{2}\right)\Lambda_{tw} \\ & + \left(\frac{C_{13}}{2} + C_{11}\frac{\mu^2}{4}\right)\theta_{ri}\ d_{1k1}\ \frac{\mu}{2}\Lambda_{1c} \qquad (6)\end{aligned}$$

$$\begin{aligned} & - 2\ d_{3k2}\ \mu\ \Lambda_0 - \left(d_{2k1} + d_{3k1}\frac{3\mu^2}{4} + d_{3k3}\right)\Lambda_{1s} \\ & + d_{1k2}\ \Lambda_{1c} + \frac{1}{2}C_{11}\mu\lambda \\ & + \left(C_{11}\frac{\mu^2}{8} - \frac{C_{13}}{2}\right)\beta_{1c} + \frac{(\nu^2 - 1)}{\gamma}\beta_{1s} \\ & - 2\ d_{3k3}\ \mu\ \Lambda_{tw} - C_{12}\ \mu\ \theta_{ri} = 0 \qquad (7)\end{aligned}$$

$$\begin{aligned} & C_{12}\frac{\mu}{2}\beta_0 - d_{1k2}\ \Lambda_{1s} - \left(d_{2k1} + d_{3k1}\frac{\mu^2}{4} + d_{3k3}\right)\Lambda_{1c} \\ & + \left(C_{11}\frac{\mu^2}{8} + \frac{C_{13}}{2}\right)\beta_{1s} + \frac{(\nu^2 - 1)}{\gamma}\beta_{1c} = 0 \qquad (8)\end{aligned}$$

Rotor Slowing Trim Formulation

The operating condition of the helicopter rotor system is determined by force and moment equilibrium of the entire vehicle. Since additional canard and tail wing lifts along with a tail propulsion are included to the vehicle configuration, longitudinal and lateral equilibrium of the new helicopter must be considered for trim calculations. At this initial stage, only the effects on the longitudial equilibriums are considered whereas canard and tail wing lifts are assumed to be symmetric or have cancelling effects in the lateral direction. This approximate trim formulation is based on the standart helicopter trim formulations given by Johnson [10].

Longitudinal force equilibrium consideres the forces in the vertical longitudial plane of the helicopter as seen in Figure 2. The helicopter has speed V_H and a flight path angle θ_{fp}, so that climb and descent conditions can be also considered. The acceleration effects of during rotor

slowing down transition are neglected and steady unaccelerated flight conditions are assumed for the formulation.

The forces on the rotor are the main rotor trust T_{mr}, and the rotor drag H are defined relative to the reference rotor hub plane. This reference plane has angle of attack α with respect to the forward speed. The forces acting on the helicopter are the weight W of the helicopter, canard and tail wing lifts, L_{can}, L_{tw}, aerodynamic drags of fuselage D_f, canard and tail wing D_{can}, D_{tw} respectively. A tail propulsion, T_{pr}, is also applied in the direction of the hub reference plane from aft rear end of the tail boom. Forces and moments acting on the helicopter are also illustrated in Figure 2. Vertical force equilibrium requirements is

$$W = T_{mr} \cos\alpha_s + H \sin\alpha_s - D_T \sin\theta_{fp} + L_T \cos\theta_{fp} - T_{pr} \sin\alpha_s. \quad (9)$$

and the horizontal force equilibrium can be written as;

$$D_T \cos\theta_{fp} + H \cos\alpha_s = T_{mr} \sin\alpha_s - L_T \sin\theta_{fp} + T_{pr} \cos\alpha_s \quad (10)$$

where,

$$D_T = D_f + D_{can} + D_{tw}$$
$$L_T = L_{can} + L_{tw}$$
$$\alpha_s = \alpha - \theta_{fp}$$

Next the equilibrium of pitch moments on the helicopter which determines the angle of attack of the rotor shaft relative to the vertical, α_S is considered. Moments are taken about the rotor hub so that the rotor forces are not involved and the rotor reference plane is not entered to the problem. The rotor hub moment M_Y must be included and the pitching moment equilibrium about the rotor hub, for small angles, can be written as,

$$M_Y + M_{YF} + W(h\sin\alpha_s - x_{cg}\cos\alpha_s) - hD_F\cos\alpha_s - x_{cg}D_F\sin\alpha_s + L'_{can}l_c - D'_{can}h_{can} - L'_{tw}l_{tw} - D'_{tw}h_{tw} + T_{pr}h_{pr} = 0 \quad (11)$$

where L' and D' are auxillary lift and drag forces relative to the rotor thrust T direction.

$$L'_{can} = L_{can}\cos\alpha - D_{can}\sin\alpha$$

$$D'_{can} = D_{can}\cos\alpha + L_{can}\sin\alpha$$

where M_{YF} is the aerodynamic pitch moment of the fuselage; h and x_{cg} are the offset distances of the helicopter center-of-gravity location in vertical and longitudinal directions respectively.

As seen from Figure 2 canard and tail wing lifts are acting from distances l_c and l_w from the main rotor shaft axis and tail propulsion is located with a distance h_{pr} below of the hub plane. Canard and tail wing surfaces are located at distances $h_{can}$and h_{tw} below the hub center. Aerodynamic drag forces of canard and tail wing surfaces are approximated as $D_{can} \approx \frac{1}{8}L_{can}$.

For given values of auxillary lift and propeller trust and the steady forward flight condition (defined by forward speed V_H and flight path angle θ_{fp}) the required amount of main rotor trust is found by equation 9 which is arranged as

$$T_{mr} = \frac{W}{\cos\alpha_s} - H\tan\alpha_s + D_T\frac{\sin\theta_{fp}}{\cos\alpha_s} - L_T\frac{\cos\theta_{fp}}{\cos\alpha_s} + T_{pr}\tan\alpha_s \quad (12)$$

Equations 10 and 11 are solved for $\beta_{1c_{HP}}$ and α_s along with equalities,

$$\frac{M_Y}{Wh} = \frac{(\nu^2-1)/\gamma}{h2C_T/\sigma a}\beta_{1c_{HP}}$$

and

$$H = H_{HP} = H_{TPP} - \beta_{1c_{HP}}$$

Newly found values of $\alpha_s, \beta_{1c_{HP}}, C_{T_{mr}}$ and β_0 represent the new trim values and the Λ_0, Λ_{1s} and Λ_{1c} are the control parameters for the flap control case.

Aerodynamic Formulation

The nonconservative generalized forces which come as a result of the aerodynamic environment are presented by Greenberg's extension of Theodorsen's theory for thin, two-dimensional airfoils undergoing unsteady motion in a time-varying incompressible free-stream. As formulated in reference [11] Theodorsen theory faciliates chordwise rigid airfoil with trailling edge flap or control surface hinged at $x_f = \frac{c}{2}c_f$. The airfoil may have a vertical translation $h(t)$ and can rotate about an axis at $x = \frac{c}{2}a$ through an angle $\alpha(t)$; and $\Lambda(t)$ donates the angular displacement of the flap relative to the airfoil chordline.

Details of the formulation of quasisteady aerodynamics of oscillating airfoil with unbalanced flap motions particularly for the rotary wing environment are given in reference [5].

Rotor Blade Nonlinear P.D.E's

Several methods have been developed for the solution of nonlinear coupled partial differential equations representing the flap-lag-torsion motions of hingeless and bearingless rotor blades. A conditionally stable, explicit finite difference scheme to numerically integrate the nonlinear blade partial differential equations in space and time has been formulated by Yillikci and Hanagud [9, 5].

For purposes of numerical integration by the proposed approach which is based on explicit finite difference methods, it is convenient to express the coupled

nonlinear partial differential equations of rotor blade system in terms of first order time and second order space derivatives. This reduction is performed by introducing the following variables.

$$\begin{aligned} \mathbf{u}_t &= \frac{\partial \mathbf{u}_d}{\partial \psi} = \frac{\partial}{\partial \psi}\{v, w, \phi\}^T, \\ \mathbf{u}_m &= \{m_v, m_w\}^T = \frac{\partial}{\partial x^2}\{v, w\}^T \end{aligned} \tag{13}$$

In terms of these variables, rotor blade nonlinear, coupled partial differential equations and the trailing terms are reorganized in matrix form as follows,

$$\begin{aligned} \overset{*}{\mathbf{u}}_t &= \bar{\mathbf{A}}(\mathbf{u}, \psi)\mathbf{u}_m^{++} + \bar{\mathbf{B}}(\mathbf{u}, \psi)\mathbf{u}_d^{++} \\ &\quad + \bar{\mathbf{C}}(\mathbf{u}, \psi)\mathbf{u}_d^{+} + \bar{\mathbf{D}}\mathbf{u}_t \\ &\quad + \bar{\mathbf{E}}(\mathbf{u}, \psi)\mathbf{u}_m + \bar{\mathbf{F}}(\psi)\mathbf{u}_d + \bar{\mathbf{g}}(\mathbf{u}, \psi) \\ \overset{*}{\mathbf{u}}_m &= \mathbf{I}_{23}\mathbf{u}_t^{++} \\ \overset{*}{\mathbf{u}}_d &= \mathbf{I}_{33}\mathbf{u}_t \end{aligned} \tag{14}$$

where $()^+ = \frac{\partial}{\partial x}, \overset{*}{()} = \frac{\partial}{\partial \psi}$. Vectors $\mathbf{u}_d$ and $\mathbf{u}_t$ are displacement and velocity vectors respectively. Details of the formulation and the conditionally stable explicit finite difference method used for numerical solutions are given in references [9, 5].

III. Results and Discussions

Since the objective of this study is to illustrate the application of introduced approximate method, certain simplifications are made. These simplifications can be outlined as;

- Uniform inflow conditions along the blade span is considered.
- Hub and tip loses are only included by reducing the blade chord dimension at root and tip of the blade.
- Reverse flow effects are not included.
- Structural and mass properties of the blade are also taken as uniform along the blade.
- All offsets from the elastic axis are assumed to be zero.

Basic vehicle and rotor blade configuration parameters for the considered 700 lb micro-helicopter are given in Table 1. Main rotor has radius R_{mr}=8.6 ft. with blade chord c=1.4 ft. Trailing edge flap has a rectangular shape with width c_f=0.36 c_{MR} and starting from r_{MR}=0.4 to r_{MR}=0.95. Rotor blade for $r_{MR} > 0.25$ has assumed to have airfoil sections. If an average rectangular blade has been considered, the average blade chord would be c_{av}= 0.86 ft. Vehicle trim and rotor response calculatons are initiated from zero forward speed and flight conditions are defined with advance ratio μ, rotor angular speed Ω for the pure helicopter forward flight conditions. Forward speed is increased from μ=0.0 to μ= 0.325 with $\Delta\mu$=.025 increments where as rotor angular speed is kept constant at its maximum value, $\Omega = 76$ rad/sec during this initial standart helicopter mode without utilization of auxillary lift and propulsion. At each flight interval change the flap controls are introduced by linear increments.

After pure helicopter configuration is reached to steady-state forward flight condition at μ =0.325, rotor slowing down transition is started by gradually introducing auxillary lift and forward propulsion. For each rotor slowing down flight interval parameters are set as;

$$\begin{aligned} \Omega_{k+1} &= \Omega_k - \Delta\Omega \\ C_{L_{k+1}} &= C_{L_k} + \Delta C_L \\ C_{PR_{k+1}} &= C_{PR_k} + \Delta C_{PR} \\ \theta_{FP_{k+1}} &= \theta_{FP_k} - \Delta\theta_{FP} \\ V_{H_{k+1}} &= V_{H_k} - \Delta V_H \end{aligned}$$

where C_L and C_{PR} are total auxillary lift and tail propulsion coefficients nondimensionalized similar as main rotor thrust coefficient $C_{T_{MR}}$,

$$C_L = \frac{L_{can} + L_{tw}}{\rho\pi\Omega^2 R^4}, \quad C_{PR} = \frac{T_{PR}}{\rho\pi\Omega^2 R^4}$$

Since blade stiffness parameters,

$$\Lambda_1 = \frac{EI_y}{m\Omega^2 R^4}, \quad \Lambda_2 = \frac{EI_z}{m\Omega^2 R^4}, \quad \Delta = \frac{GJ}{m\Omega^2 R^4}$$

are nondimensionalized with rotor angular speed they are updated with the new Ω_{k+1} at kth flight interval. Since blade nondimensional stiffness parameters are changed significantly ($\Lambda_{1_{\Omega=40}} = 4\Lambda_{1_{\Omega=80}}$), time step Δt of the conditionally stable explicit finite difference scheme is also checked and changed based on the numerical stability criteria of the numerical scheme.

Trim results are obtained for five different flight conditions. Case 1 represents slowing down rotor for pure helicopter configuration with no auxillary lift and propulsion and controlled by standart pitch control. Level speed is decreased by ΔV_H =1.0 ft/sec for each $\Delta\Omega$ =1.0 rad/sec rotor rpm reduction while the stopped rotor is assumed to be descending with $\Delta\theta_{fp}$ =0.003 rad for each rotor rpm drop. Second case, Case 2 is for the case where stopped rotor is controlled by flap control and for this case helicopter is utilized with canard and tail wings with lift increments ΔC_L = 4.0E-5 at each interval. Case 3 is the first case where tail propulsion is introduced with increments ΔC_{PR} =3.0E-5. Level speed of the helicopter has kept constant at its highest value reached during

Number of blades	$b = 2$
Main rotor radius	R_{MR} = 8.6 ft
Main rotor speed	Ω_{MR} = 76 rad/sec
Main chord	c_{MR}= 1.4 ft
Flap width	c_f= 0.36 c_{MR}
Hub offsets	x_{cg}= 0.125 ft
	h=1.8 ft
Canard position	l_{can} =0.6R_{MR}
	h_{can}=3.0ft
Tail wing position	l_{tw} =0.6 R_{MR}
	h_{tw}=1.2ft
	h_{pr}=1.0 ft
Gross weight	W_g= 700 lb
First lag frequency :	Λ_2=0.04
First flap frequency :	Λ_1 =0.0306
First torsion frequency :	Δ=0.1
Cross sectional inertias	$\left(\frac{k_A}{k_M}\right)^2 = 1.0$
	$\left(\frac{k_M}{R}\right) = .025$
	$\left(\frac{k_{m_1}}{k_{m_2}}\right) = 0.0$
Drag coefficient :	C_{D0}=0.01
Solidity ratio :	σ=0.066
Lock number :	γ=6.
2-D Lift curve slope :	$a = 2\pi$
Advance ratio	μ, variable
Blade rigid pitch	θ_{ri} = 0.10 rad
Blade pretwist angle	θ_{tw} = -.05 rad

Table 1: Stop Rotor Blade and Vehicle Configuration Parameters for Flap-Lag-Torsion Motions in Forward Flight

	ΔC_{L_T}	$\Delta C_{T_{pr}}$	ΔV_H (ft/sec)
CASE 1	0.0	0.0	1.0
CASE 2	4.0E-5	0.0	1.0
CASE 3	4.0E-5	3.0E-5	1.0
CASE 4	6.0E-5	3.0E-5	0.0
CASE 5	6.0E-5	3.0E-5	0.0

Table 2: Flight Parameters, $\Delta\theta_{fp}$ =0.003 rad and $\Delta\Omega$ = 1.0 rad/sec

initial pure helicopter mode. In Case 5, auxillary lift increment is ΔC_L =6.0E-5 along with the same amount of tail propulsion as used in Cases 3 and 4. Case 5 a is constant level speed flight with highest level of auxillary lift and propulsion utilization. Descending flight condition is also considered for Case 5.

Results of trim calculations are presented in Figures 3 and 4 for five considered slowing down flight conditions. Figure 3 shows the main rotor power requirement and the main rotor thrust variation for the considered cases. Highest main rotor thrust and power levels are obtained for the pure helicopter configuration whereas additional lift and propulsion have significantly reduced main rotor loads as seen from Figure 3.

Rotor control inputs and vehicle angle of attack has variation with forward speed have shown in Figure 4. For the pure helicopter case, Case 1, control input is the combination of collective and cyclic pitch and for all other cases flap controls are used. Since a rigid pitch angle is also used for flap controlled rotors, the required collective pitch is higher than the collective flap. For Case 2 where only auxillary lift has been used, the amount of collective flap is out of practical applicable levels as well as for the pitch controlled case. For Cases 3-5 tail propulsion significantly reduced the collective flap input requirement. Similar effects are also observed for cyclic flap inputs. As also seen from Figure 4, vehicle angle of attack has reduced for flap controlled compound configurations. Flight parameters are also outlined in Table 2.

Rotor blade nonlinear elastic deflections are calculated and results are given for tip vibrations in Figures 5 and 6 as sections captured from transient vibrations where rotor rpm reduction and related control inputs are introduced as step functions. In Figure 5 elastic tip deflections for Cases 2, 3 and 5 are given for rotor speed Ω = 66. rad/sec. As seen from figure, amount of trailing edge flap motions are closely related with the level of applied auxillary lift and propulsion. For Case 2 where only additional lift is used, the amount of flap control found to be too high for a practical application. Tip deflections also show differences for the considered cases whereas lowest vibration levels are observed for Case 5 which also represents the most desirable flight condition.

Similar results are given for Ω = 40. rad/sec in Figure 6 and flap control for Case 2 is completely out of practical levels. Flap and torsional vibrations are close with each other for Cases 3 and 5 but lead-lag vibrations found to be higher for Case 5.

Last set of results are obtained for transient blade tip responses for a faster slowing down rotor obtained for Case 5 trim solutions. Flight conditions and the corresponding blade controls are changed through 2-3 blade revolutions, faster as the blade slowed down. Flap con-

trol input variation and blade elastic tip deflections are illustrated in Figure 8. As seen from figure, elastic flap and twist tip deflections started to have higher harmonics as the rotor rpm reduced.

IV. Conclusions and Remarks

Since the major objective of this study was to develop a numerical tool to calculate elastic blade response for rotor slowing down transition mode, a specific emphasis was not given for the search and design of a particular blade or helicopter configuration. A systematic study must be done for a clear understanding of the blade transition dynamics and for the proper selection of blade stiffness and mass properties for a stable stopped/flipped rotor configuration. The approximate trim formulation found to be efficient for overall performance evaluations and trim solutions obtained for torsionally stiff configurations are within the accuracy of conventional pitch control trim calculations.

The aerodynamic formulation for the unsteady oscillating rotor blade airfoil with trailing edge flap controls and conditionally stable explicit finite difference scheme is found to be an effective method for response calculations. With the use of paralel computing hardware and software capabilities of today's computer technologies it is also believed that this method can be also developed as an efficient tool for dynamic simulation of advanced rotorcraft blades with High Harmonic Control and Individual Blade Control features.

Based on these observations, present study is planned to be extended with new formulations such as;

- Vehicle trim formulation including lateral equilibrium requirements and differential canard and tail wing lift applications.
- Elastic trim formulations for a better modeling of lift variations due to the elastic deformation especially twist of the blade.
- Including flight constain and/or objective functions defining the desired or required optimum transition flight conditions.

References

[1] Strehlow, H.; and Rapp, H.: "Smart materials for Helicopter Rotor Active Control", AGARD CP-531, April 1993.

[2] Lemnios, A.Z.; and Jones, R.: "The Servo Flap- An Advanced Rotor Control System", Presented at the AHS Design Specialist Meeting on Vertical Lift Aircraft Design, San Francisco, California, 17-19 January 1990.

[3] Phillips, N.B.; and Merkley, D.J.: " BHTI's Technical Assessment of Advanced Rotor and Control Concepts", Presented at the AHS Design Specialists' Meeting on Vertical Lift Aircraft Design, San Francisco, California, 17-19 January 1990.

[4] Straub, F.K.; and Merkley, D.J.: " MDHC's Technical Assessment of Advanced Rotor and Control Concepts", Presented at the AHS Design Specialists' Meeting on Vertical Lift Aircraft Design, San Francisco, California, 17-19 January 1990.

[5] Yillikci, Y.K.; Hanagud, S.V.; Schrage, D.P.; Higman, J.: " Aeroelastic Analysis of Rotor Blades With Flap Control", Presented at the 18th European Rotorcraft Forum, September 15-18 1992, Avignon, France.

[6] Rutherford, J.W.; O'Rouke, M.J.; Lovenguth, M.A.; and Mitchell, C.A.: "Concept Assessment of Two High Speed Rotorcraft", Journal of Aircraft, Vol. 30, No:2, March-April 1993, pp 241-247.

[7] Blanchette, B.M.: "Design and Construction of A Ship Launched VTOL Unmanned Air Vehicle, Thesis, Naval Postgraduate School, Monterey CA, June 1990.

[8] Kisli, E.; Prasad, J.V.R.; Yillikci, Y.K.: "Conceptual Design of A Stopped Rotor With Flap Controls", Presented at the 18th European Rotorcraft Forum, September 15-18 1992, Avignon, France.

[9] Yillikci, Y.K., Prasad, J.V.R., and Schrage, D.P.: "Blade Response Simulations of Flap Controlled Stopped Rotors", Forum Proceeding, AIAA International Powered Lift Conference, 1-3 December 1993, San Francisco, USA.

[10] Johnson, W.: *Helicopter Theory*, ch.2 Princeton, 1980.

[11] "Bishlinghoff, R.L.; Asley, H; Halfman, R.L.: *Aeroelasticity*, Addison Wesley Publishing Company, 1975.

[12] Yillikci, Y.K.; and Hanagud, S.V.: "Finite Difference Techniques and Rotor Blade Aeroelastic Partial Differential Equations: An Explicit Time-Space Finite Element Approach For P.D.E.", Presented at the 15th European Rotorcraft Forum, September 12-15, 1989, Amsterdam, Netherlands.

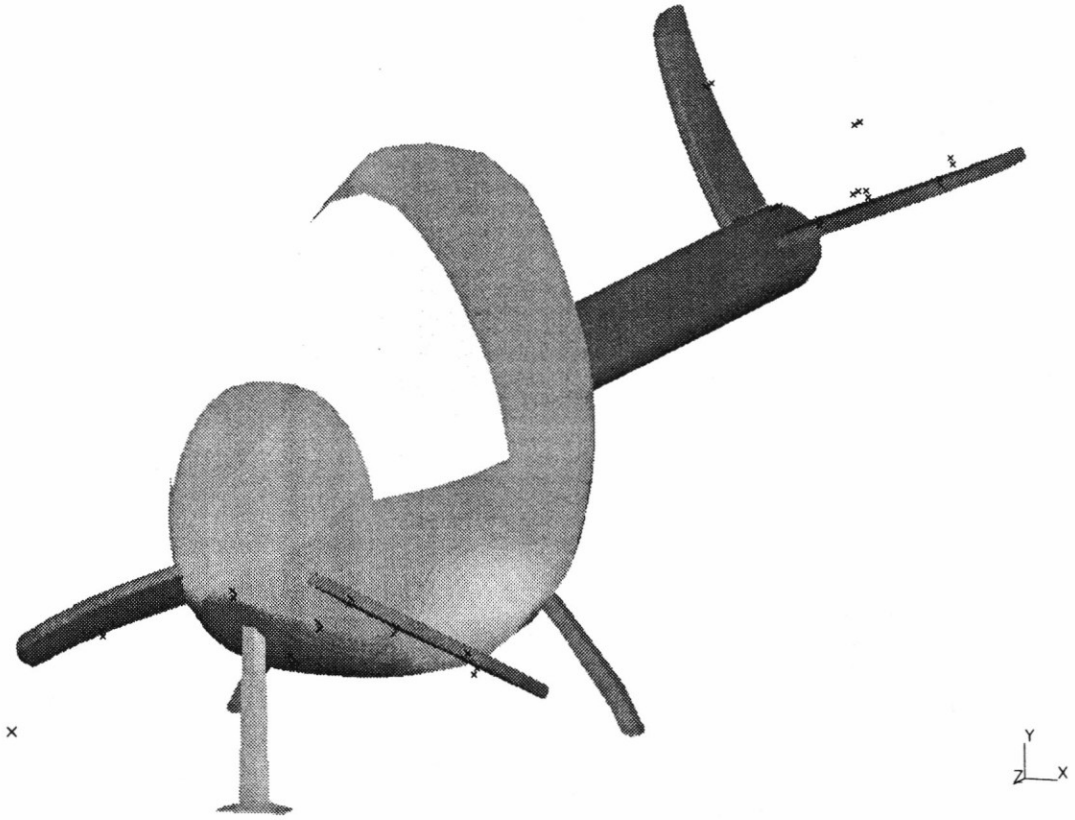

Figure 1. ANKA-1 Micro Stopped Rotor General Configuration.

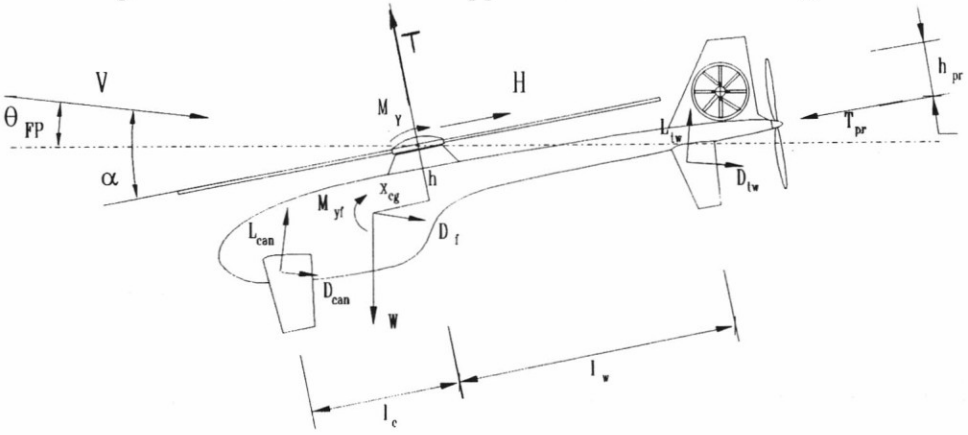

Figure 2. Longitudinal Force and Moment Equilibrium of Stopped Rotor.

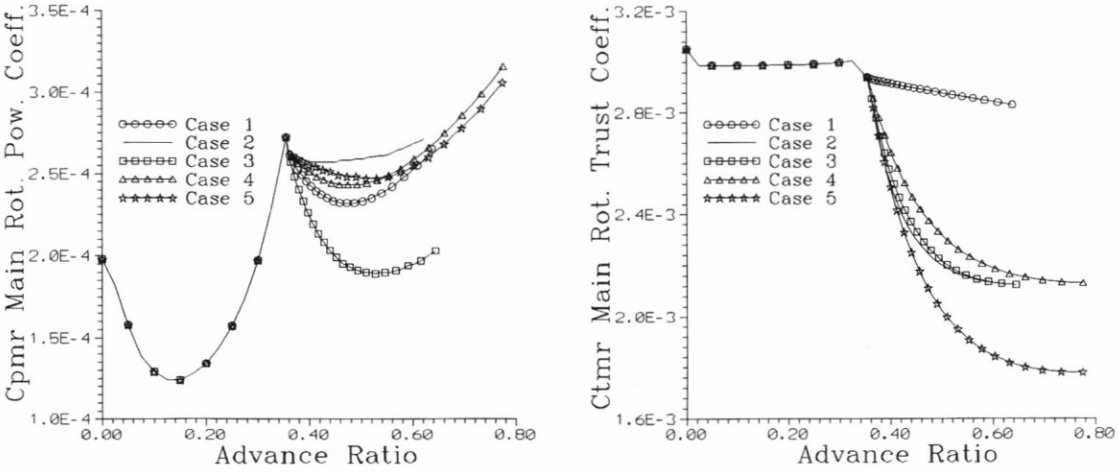

Figure 3. C_{pmr} and C_{tmr} Variations For Different Configurations.

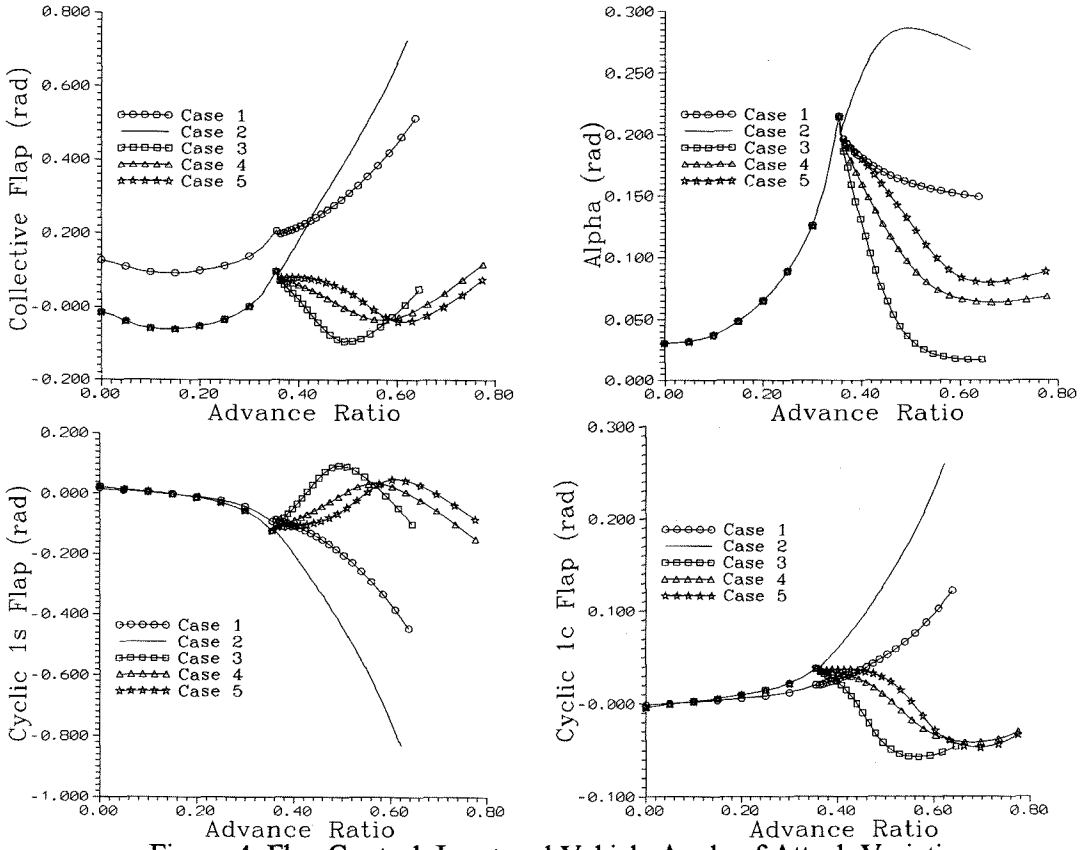

Figure 4. Flap Control Input and Vehicle Angle of Attack Variation.

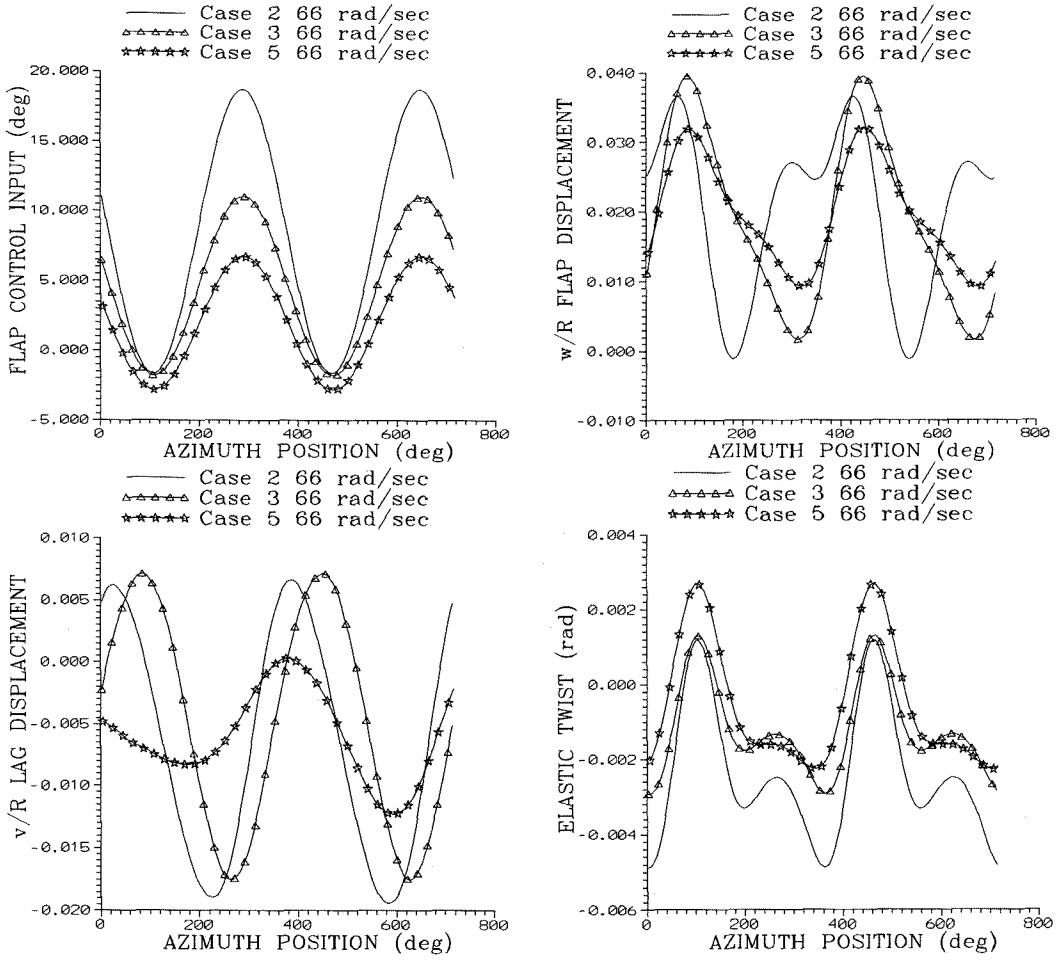

Figure 5. Elastic Blade Tip Responses For Cases=2, 3 and 5 (Ω=66. rad/sec).

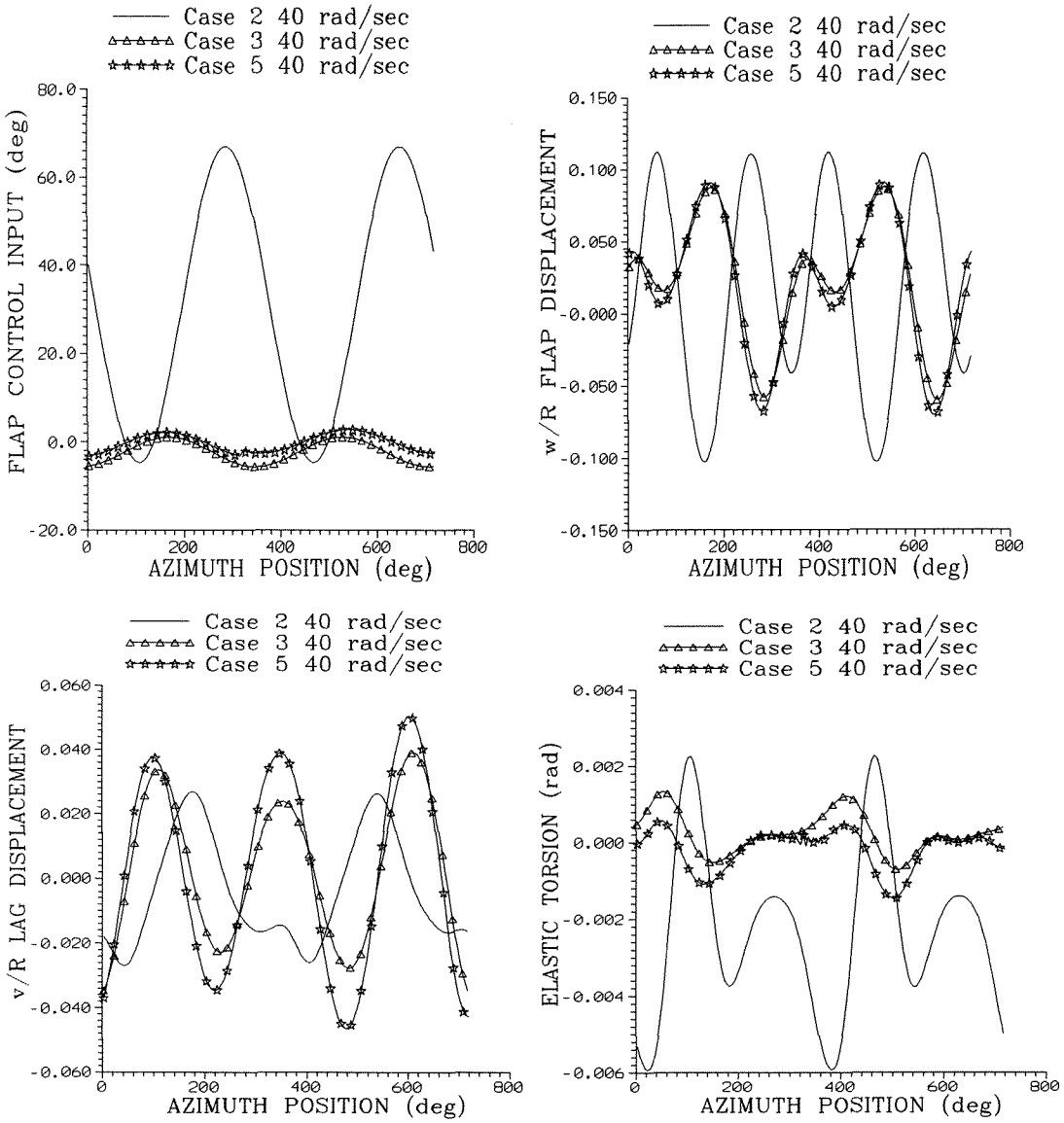

Figure 6. Elastic Blade Tip Responses For Cases=2, 3 and 5 (Ω=40. rad/sec).

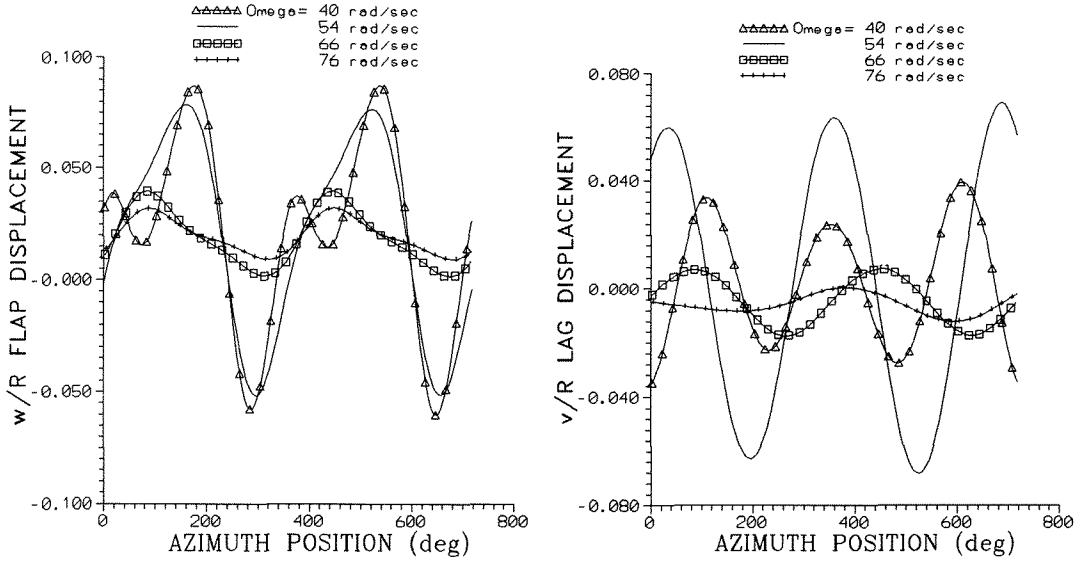

Figure 7. Elastic Blade Tip Responses For Different Rotor Speeds (Case 5).

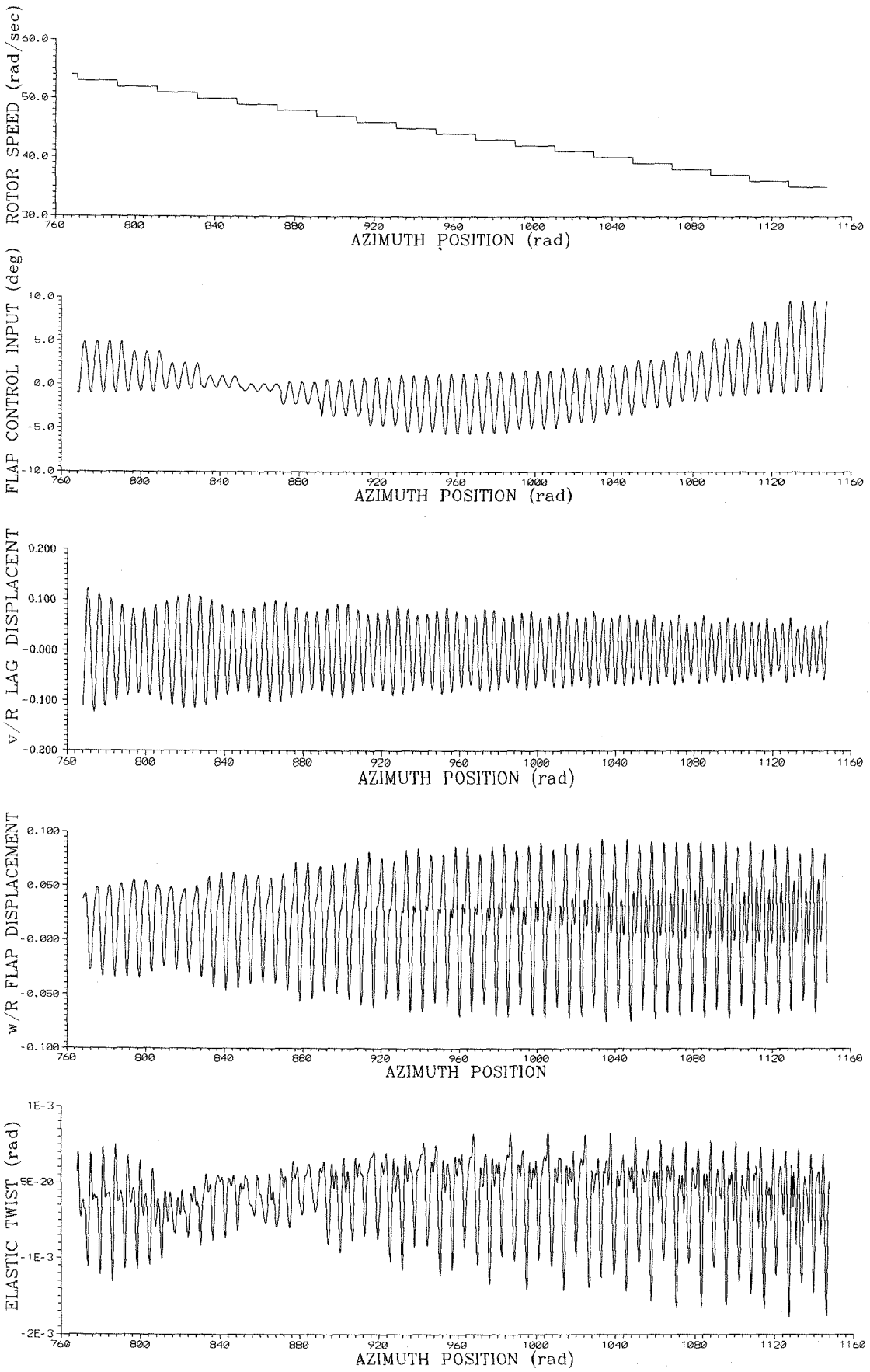

Figure 8. Transient Blade Tip Deflections For Case 5.